A novel paramagnetic dithiadiazolyl radical: Crystal structure and magnetic properties of *p*-$BrC_6F_4CNSSN^{\bullet}$

Guillermo Antorrena,[a] John E. Davies,[b] Matthew Hartley,[b] Fernando Palacio,[a] Jeremy M. Rawson,*[b] J. Nicholas B. Smith[b] and Alexander Steiner[c]

[a] *Instituto de Ciencia de Materiales de Aragon, CSIC-Universidad de Zaragoza, Zaragoza, Spain E-50009*
[b] *Department of Chemistry, The University of Cambridge, Lensfield Road, Cambridge, UK CB2 1EW. E-mail: jmr31@cam.ac.uk*
[c] *Department of Chemistry, The University of Liverpool, Crown Street, Liverpool, UK L69 7ZD*

Received (in Cambridge, UK) 11th May 1999, Accepted 8th June 1999

The dithiadiazolyl radical *p*-$BrC_6F_4CNSSN^{\bullet}$ 2 retains its monomeric nature in the solid state; variable temperature magnetic studies on 2 indicate Curie–Weiss behaviour (θ = −27 K) above 60 K with an effective magnetic moment of 1.45 μ_B at room temperature; the absence of long-range magnetic order down to 1.8 K is attributed to the low dimensionality of the magnetic exchange pathway predicted on the basis of the inter-molecular S···N interactions.

The magnetic properties of the dithiadiazolyl radical *p*-NCC_6F_4CNSSN **1** are exceptional.[1,2] The β-phase of this compound is one of a small number of organic magnets and it exhibits a magnetic ordering temperature (36 K) unprecedented for an organic radical.[2] The singly-occupied molecular orbital (SOMO) of **1**, as with other dithiadiazolyl derivatives,[3] is a π-based orbital of a_2 symmetry (nodal at C) and is localised on the heterocyclic ring. Thus, to a first approximation, we may assume that variation of the substituent at C will have only minor effects on the electronic properties of the radical centre. Indeed, because of these negligible electronic effects, one of the most difficult tasks associated with this particular area of chemistry is to overcome the considerable dimerisation energy (*ca.* 35 kJ mol^{-1})[3] associated with these radicals. In **1**, a fortuitous combination of the fluorinated aromatic ring, coupled with strong CN···S interactions effectively compete with the natural tendency for spin-paired dimerisation.[1,2]

Recently, we have concentrated our efforts on a series of fluorinated derivatives, closely related to **1**. Herein, we report the synthesis and structure of *p*-BrC_6F_4CNSSN **2**, which represents only the second example of a dithiadiazolyl radical to retain its paramagnetic nature in the solid state.

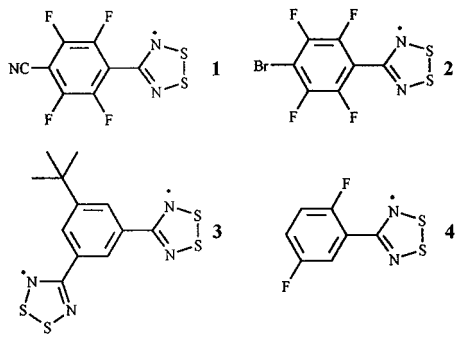

Radical **2** was prepared from BrC_6F_4CN using standard synthetic procedures[4] and was purified by vacuum sublimation (10^{-2} Torr, 80 °C), with recovered yields typically 14%, based on *p*-BrC_6F_4CN. Red crystals suitable for X-ray diffraction† were obtained by successive sublimations along a glass tube under dynamic vacuum.

The asymmetric unit (Fig. 1) comprises one molecule of **2** of unexceptional geometry, and with a large twist angle between C_6 and CN_2S_2 rings of 51.8° (*c.f.* α-**1** and β-**1** at 32° and 58°, respectively).[1,2] The majority of dithiadiazolyl radicals are associated *via* a close out-of-plane interaction between the two heterocyclic rings with S···S separations of 2.9–3.1 Å,[5] which facilitates at π*–π* interaction between the singly occupied molecular orbitals (SOMOs) based on each heterocyclic ring, thereby rendering them diamagnetic. In **2** the radicals pack in columns along the crystallographic *a*-axis (Fig. 2), although these out-of-plane contacts are much longer than normal out-of-plane contacts and fall in the range 3.675–3.999 Å, larger than those observed for the bis(dithiadazolyl) radical **3** [3.48(2)–3.61(2) Å][8] and the fluorinated dithiadiazolyl radical **4** [3.544(3) Å].[9] Whilst the molecular structures of **1** and **2** are similar, their solid state structures are different; radical **1** forms a chain-like motif through electrostatic CN···S interactions.[1,2] In the case of **2** the difference in electronegativity between Br and S (0.04) is much less than that observed between S and an sp-hybridised N (2.49) in **1**. Instead electrostatic interactions between S and the heterocyclic sp^2 N (electronegativity

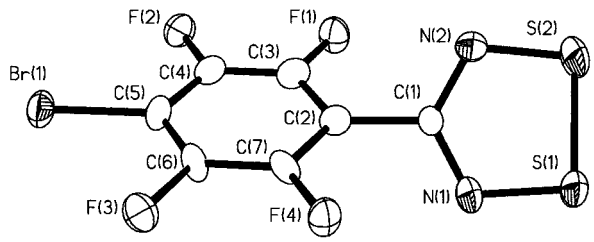

Fig. 1 Selected intramolecular bond lengths (Å) and angles (°) for **2**: S(1)–S(2) 2.070(4), S(1)–N(1) 1.640(8), S(2)–N(2) 1.624(9), C(1)–N(1) 1.317(14), C(1)–N(2) 1.327(12), N(1)–S(1)–S(2) 93.7(4), N(2)–S(2)–S(1) 95.5(3), C(1)–N(1)–S(1) 113.9(7), C(1)–N(2)–S(2) 112.8(7), N(1)–C(1)–N(2) 124.0(9).

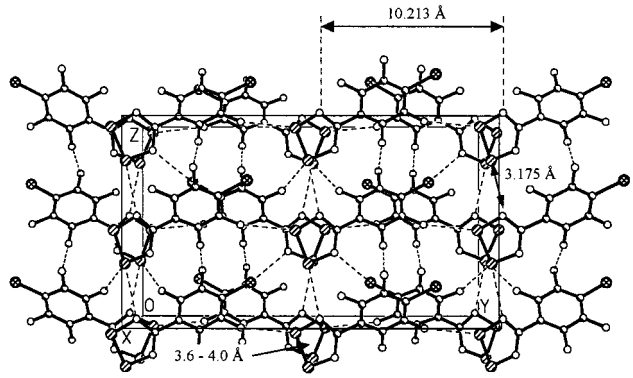

Fig. 2 Molecular packing diagram of **2** viewed perpendicular to the crystallographic *a*-axis, with selected intermolecular contacts labelled (see text for discussion).

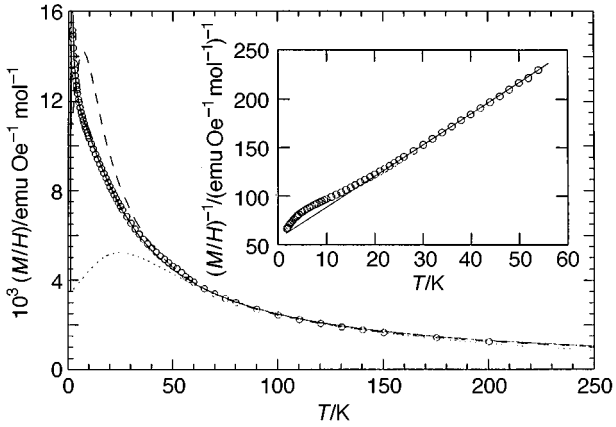

Fig. 3 Variation of M/H as a function of T (○) for **2** and several fits to modified Bonner–Fisher models: Bonner–Fisher with an additional diamagnetic term (·····); Bonner–Fisher considering that only 70% of the molecules contribute to the magnetism (-----) $J = -5.4(1)$ K; and Bonner–Fisher including a linear dependence $J(T)$ term and a paramagnetic term (——).

difference = 1.55) determine the crystal packing. This is manifested in a short intermolecular interaction [S(1)···N(2) 3.175(9) Å] close to the heterocyclic ring plane which links neighbouring molecules into chains along the *c*-axis. Whereas out-of-plane contacts around 3.0 Å lead to essentially diamagnetic solids, this close in-plane approach in **2** leads to retention of paramagnetism (see below).

Variable temperature magnetic susceptibility studies (ac and dc) under different applied magnetic fields were carried out on a microcrystalline sample of **2**. Diamagnetic corrections, were made for the sample holder and sample (Pascal's constants). The effective magnetic moment at high temperature [μ_{eff} = 1.45 μ_B at room temperature] is less than that expected for an $S = ½$ paramagnet and decreases slowly to 1.35 μ_B at 50 K before undergoing a more rapid decrease down to 0.5 μ_B at 1.8 K.

Above 60 K, the magnetic susceptibility follows the Curie–Weiss law with $\theta = -27 \pm 1$ K (Fig. 3, inset), although an extra and unjustified diamagnetic term ($\chi_d \approx -5 \times 10^{-4}$ emu mol^{-1}) must be added in order to explain the low values of μ_{eff}. Using a mean-field approximation, this value of θ would indicate a paramagnetic–antiferromagnetic phase transition at 27 K. However no evidence of long range magnetic order is observed and the linear field dependence of the susceptibility is corroborated at 5 K by a magnetisation *vs.* field plot.

On the other hand, for systems exhibiting low dimensional character (which is strongly suggested by the structure of **2**), a fit of the experimental data to the Bonner–Fisher model for an $S = ½$ Heisenberg chain gives $J = -19 \pm 5$ K and approximately the same χ_d term. This model predicts a broad maximum in χ at $T_{max} = 1.282 \times |J|$ K (24 ± 6 K), as a consequence of short range (low-dimensional) interactions (Fig. 3). However there is no broad maximum in χ observed down to 1.8 K and there is a marked deviation from the Bonner–Fisher model below 60 K. It has not been possible to fit the experimental data satisfactorily by simply including paramagnetic impurities or correction factors due to hypothetical sample degradation (Fig. 3).

These observations indicate a peculiar evolution of the susceptibility as a function of temperature, exhibiting paramagnetic behaviour with antiferromagnetic interactions ($J > 19$ K) in the high temperature range and weaker interactions at low temperatures. However, a surprisingly good fit is obtained throughout the temperature range by incorporating a simple linear dependence of the exchange parameter, J_2 [$J = -(0.31T + 8.2)$] in the Bonner–Fisher model (Fig. 3). In this case, there is no need to use an extra diamagnetic correction, although an additional paramagnetic term (corresponding to 3% of $S = ½$ paramagnetic impurity) is included to explain the large slope of the susceptibility below 10 K.

The absence of a transition to a magnetically ordered state must arise as a consequence of the crystal structure which necessarily precludes propagation of the magnetic exchange interaction throughout the solid above 1.8 K (the limiting low temperature of these measurements). The structure of **2** provides two potential pathways for propagation of the magnetic exchange interaction; either *via* the close in-plane interactions along the crystallographic *c*-axis; and/or *via* the out-of-plane interactions along the crystallographic *a*-axis (Fig. 2). Whilst the intermolecular S···N interactions in β-**1** lead to a diamond-like three-dimensional magnetic exchange pathway,[10] the dimensionality of **2** could, at best, be described as a two-dimensional net with layers separated by half the length (10.213 Å) of the crystallographic *b* axis. Thus the peculiar behaviour of *J* can be ascribed to either structural changes as the temperature decreases,[11] or to the presence of competing ferromagnetic and antiferromagnetic exchange interactions. In the first case, the temperature dependence of *J* will be a direct consequence of the modification of the exchange pathways, whereas in the second case it would just be a mathematical artefact to account for the rising of the magnetisation due to the ferromagnetic interactions. In order to provide a more solid basis to resolve this problem, low temperature structure determinations are in progress.

We would like to thank Ciba-Geigy and the MEC for studentships (J. N. B. S. and G. A., respectively), the Royal Society for an equipment grant (J. M. R.), the CICYT (Grant No. MAT94-043 and MAT97-0951), the British Council and the MEC for their support of international cooperation (J. M. R./F. P.).

Notes and references

† *Crystal data* for **2**: $C_7BrF_4N_2S_2$, $M = 332.12$, orthorhombic, space group *Aba*2, $a = 8.263(2)$, $b = 20.426(4)$, $c = 11.556(2)$ Å, $U = 1950.4(7)$ Å^3, $Z = 8$, $D_c = 2.262$ g cm^{-3}, $\lambda = 0.71073$ Å, $T = 150(2)$ K, μ(Mo-Kα) = 4.672 mm^{-1}, $F(000) = 1272$. Data were collected on a Rigaku AFC-7 four-circle diffractometer using an oil-coated rapidly cooled crystal of dimensions 0.35 × 0.25 × 0.20 mm using the ω–2θ method ($3.17 \leqslant \theta \leqslant 27.51°$). Of a total of 2292 collected reflections, 2175 were independent (R_{int} = 0.0449). The structure was solved by direct methods[5] and refined using full-matrix least squares[6] on F^2 to final values of R_1 [$F > 4\sigma(F)$] = 0.0643 and wR_2 = 0.1428 (all data), goodness of fit = 1.026; largest peak and hole in the final difference map were within +0.91, −0.59 e Å^{-3}; the refined Flack parameter [−0.02(2)] indicates the correct absolute structure.[7] CCDC 182/1279. See http://www.rsc.org/suppdata/cc/1999/1393/ for crystallographic files in .cif format.

1 A. J. Banister, N. Bricklebank, W. Clegg, M. R. J. Elsegood, C. I. Gregory, I. Lavender, J. M. Rawson and B. K. Tanner, *J. Chem. Soc., Chem. Commun.*, 1995, 679.
2 A. J. Banister, N. Bricklebank, I. Lavender, J. M. Rawson, C. I. Gregory, B. K. Tanner, W. Clegg, M. R. J. Elsegood and F. Palacio, *Angew. Chem., Int. Ed. Engl.*, 1996, **35**, 2533.
3 J. M. Rawson, A. J. Banister and I. Lavender, *Adv. Heterocycl. Chem.*, 1995, **62**, 137.
4 C. M. Aherne, A. J. Banister, I. B. Gorrell, M. I. Hansford, Z. V. Hauptman, A. W. Luke and J. M. Rawson, *J. Chem. Soc., Dalton Trans.*, 1993, 967.
5 SHELXS, G. M. Sheldrick, *Acta. Crystallogr., Sect. A.*, 1990, **46**, 467.
6 SHELXL 93, G. M. Sheldrick, University of Göttingen, 1993.
7 H. D. Flack, *Acta. Crystallogr., Sect. A.*, 1983, **39**, 876.
8 R. A. Beekman, R. T. Boeré, K. H. Moock and M. Parvez, *Can. J. Chem.*, 1998, **76**, 85.
9 A. J. Banister, A. S. Batsanov, O. G. Dawe, P. L. Herbertson, J. A. K. Howard, S. Lynn, I. May, J. N. B. Smith, J. M. Rawson, T. E. Rogers, B. K. Tanner, G. Antorrena and F. Palacio, *J. Chem. Soc., Dalton Trans.*, 1997, 2539.
10 P. J. Langley, J. M. Rawson, J. N. B. Smith, M. Schuler, A. Schweiger, F. Palacio, G. Antorrena, C. Hoffmann, G. Gescheidt, A. Quintel, P. Rechsteiner, R. Bachmann and J. Hulliger, *J. Mater. Chem.*, 1999, 1431.
11 A recent example of the effects of a second-order structural phase transition in a molecular magnetic compound can be found (L. R. Falvello, M. A. Hitchman, F. Palacio, I. Pascual, A. J. Schultz, H. Stratemeier, M. Toms, E. P. Urriolabeitia and D. M. Young, *J. Am. Chem. Soc.*, 1999, **121**, 2808.

Communication 9/03771C